Diagnostic and Prognostic Value of Human Prion Detection in Cerebrospinal Fluid

Aaron Foutz, MSc,[1] Brian S. Appleby, MD,[1,2,3,4] Clive Hamlin, PhD,[1,2]
Xiaoqin Liu, BSc,[1] Sheng Yang, MSc,[3] Yvonne Cohen, BSc,[1] Wei Chen, BSc,[1]
Janis Blevins, BSc,[1] Cameron Fausett, MSc,[3] Han Wang, MD, MPH,[3]
Pierluigi Gambetti, MD,[1] Shulin Zhang, MD,[2] Andrew Hughson, MSc,[5]
Curtis Tatsuoka, PhD,[3] Lawrence B. Schonberger, MD, MPH,[6]
Mark L. Cohen, MD,[1,2] Byron Caughey, PhD,[5] and Jiri G. Safar, MD[1,2,3]

Objective: Several prion amplification systems have been proposed for detection of prions in cerebrospinal fluid (CSF), most recently, the measurements of prion seeding activity with second-generation real-time quaking-induced conversion (RT-QuIC). The objective of this study was to investigate the diagnostic performance of the RT-QuIC prion test in the broad phenotypic spectrum of prion diseases.

Methods: We performed CSF RT-QuIC testing in 2,141 patients who had rapidly progressive neurological disorders, determined diagnostic sensitivity and specificity in 272 cases that were autopsied, and evaluated the impact of mutations and polymorphisms in the *PRNP* gene, and type 1 or type 2 human prions on diagnostic performance.

Results: The 98.5% diagnostic specificity and 92% sensitivity of CSF RT-QuIC in a blinded retrospective analysis matched the 100% specificity and 95% sensitivity of a blind prospective study. The CSF RT-QuIC differentiated 94% of cases of sporadic Creutzfeldt–Jakob disease (sCJD) MM1 from the sCJD MM2 phenotype, and 80% of sCJD VV2 from sCJD VV1. The mixed prion type 1-2 and cases heterozygous for codon 129 generated intermediate CSF RT-QuIC patterns, whereas genetic prion diseases revealed distinct profiles for each *PRNP* gene mutation.

Interpretation: The diagnostic performance of the improved CSF RT-QuIC is superior to surrogate marker tests for prion diseases such as 14-3-3 and tau proteins, and together with *PRNP* gene sequencing the test allows the major prion subtypes to be differentiated in vivo. This differentiation facilitates prediction of the clinicopathological phenotype and duration of the disease—two important considerations for envisioned therapeutic interventions.

ANN NEUROL 2017;81:79–92

Human prion diseases are highly heterogeneous and invariably fatal neurological disorders. They include Creutzfeldt–Jakob disease (CJD), kuru, Gerstmann–Sträussler–Scheinker disease (GSS), and fatal familial insomnia (FFI).[1] Sporadic CJD (sCJD) accounts for 85% of all cases of human prion disease; genetic CJD (gCJD) for 10–15%; and infection from exogenous sources, most frequently iatrogenic CJD, for <1%.[1,2] Prions propagate by a process in which the pathogenic prion protein (PrP^Sc) replicates exponentially by templating the misfolding of normal cellular prion protein (PrP^C).[3]

The diversity of prion diseases is further increased by distinct strains of prions that transmit a particular disease phenotype, including incubation time, clinical signs, progression rate, and patterns of PrP^Sc deposition and neuropathological lesions.[4–10] Distinct phenotypes of human

prions have been classified according to their clinicopathological characteristics, the methionine (M) or valine (V) polymorphism in codon 129 of the prion protein (PrP) gene *PRNP*, and the mass (21 or 19kDa, as type 1 or type 2, respectively) of the deglycosylated, protease-resistant PrP^{Sc} fragment.[1,11]

Apart from brain biopsy, which with more sensitive detection of PrP^{Sc} by conformation-dependent immunoassay (CDI) can reach 100% sensitivity and high specificity,[12] but carries inherent risks,[13] there is no disease-specific antemortem diagnostic test for sCJD; consequently, a definitive diagnosis of prion disease relies on postmortem detection of PrP^{Sc} in brain tissue.[1,12,14] Although technological advancements such as fluid-attenuated inversion recovery, diffusion-weighted imaging, and apparent diffusion coefficient improved both the negative and positive predictive value of brain magnetic resonance imaging (MRI) and became important tools in differential diagnostics of human prion diseases, the origin of detected patterns and relationship to deposits of pathogenic PrP^{Sc} remain unclear.[1,12,15,16] Moreover, surrogate markers that have been proposed for use in diagnostic tests for prion diseases—including the 14-3-3, S-100, and tau proteins in cerebrospinal fluid (CSF)—are released into the CSF as a result of any acute neuronal damage[17–22] and thus have low diagnostic specificity, often with contradictory indications in the same patient.[17,20,23]

These difficulties prompted us and other researchers to search for methods having high analytical sensitivity and specificity, which could detect prions directly in tissues and body fluids, and which could therefore be an accurate antemortem diagnostic test for prion diseases. Several techniques were introduced that exploit the self-replicating (seeding) power of misfolded pathogenic PrP^{Sc} for detection.[24–26] The real-time quaking-induced conversion test (RT-QuIC) uses recombinant PrP as a substrate to amplify very small amounts of PrP^{Sc} seed in CSF of CJD patients to detectable levels.[27,28] The recent use of shorter fragments of PrP as a substrate, and replacement of Western blot (WB)[29] or CDI[30] detection of the conversion reaction product with real-time monitoring of the amplification time course by a fluorescent dye, thioflavin T (ThT), resulted in a faster and more sensitive second-generation RT-QuIC.[31] This improved technique paved the way for higher diagnostic throughput in detecting human prion diseases using CSF. Here we describe the diagnostic specificity and sensitivity of human prion detection with the second-generation CSF RT-QuIC in a blinded retrospective, as well as prospective analysis of a cohort of patients suffering from diverse rapidly progressive neurodegenerative disorders and suspected of having prion disease. We compare the results with detailed neuropathological and genetic assessments and analyze the impact of disease duration, phenotype, molecular characteristics of human prions, and polymorphism of codon 129 of the *PRNP* gene on CSF RT-QuIC in sporadic and genetic prion diseases.

Subjects and Methods

Ethics Statement

All procedures were performed under protocols approved by the institutional review board at Case Western Reserve University. In all cases, written informed consent for research was obtained from the patient or legal guardian and the material used had appropriate ethical approval for use in this project. All patient data and samples were coded and handled according to NIH guidelines to protect patient identities.

Patients and Clinical Evaluations

As part of the National Prion Disease Pathology Surveillance Center (NPDPSC) protocol, medical record information is requested from clinicians who refer subjects to the Autopsy Program. Clinical records of prion disease cases were reviewed by a clinician familiar with prion disease (B.S.A.) and non–prion disease cases were reviewed by B.S.A. and C.F. Demographic data were collected using a standardized abstraction instrument and included approximate month of disease onset as documented in the medical record, gender, date of birth, date of death, clinical symptoms during the disease course, and diagnostic study results. Clinical symptoms pertaining to updated diagnostic criteria for sCJD were included.[15] Akinetic mutism was omitted due to its end-stage manifestation and commonality among cases. Brain MRIs were considered positive if the neuroradiologist's reading fulfilled the criteria as previously defined.[27] Age was calculated as age at the time of death. Data were entered into a database and analyzed via SPSS 22 (IBM, Armonk, NY).

The criteria for inclusion were (1) availability of a clinical diagnosis of CJD according to World Health Organization criteria[15,32–34] and clearly determined and dated initial symptoms upon neurological examination to ascertain the disease duration; (2) methionine or valine at codon 129 of the human PrP gene (*PRNP*); (3) unequivocal classification of type 1, type 2, or type 1-2 sPrP^{Sc} sCJD according to WB pattern; and (4) unequivocal classification of pathology as definite type 1, type 2, or mixed type 1-2 at the NPDPSC in Cleveland, Ohio.

In all cases in which neuropathology, WB, and *PRNP* gene sequencing of brain tissue excluded prion disease, we used for final diagnosis standard clinical and neuropathology protocols we published previously.[23,35] The criteria for diagnosis of rapidly progressive Alzheimer disease (AD)[35] were as follows: (1) probable clinical diagnosis of AD[35,36]; (2) absent autosomal dominant pattern of dementia; and (3) unequivocal classification as AD after detailed neuropathology and immunohistochemistry of tau proteins and amyloid beta using the current National Institute of Aging–Alzheimer's Association guidelines for neuropathological diagnosis of AD. That also included assessments of other comorbidities that could contribute to cognitive decline, including Lewy body/alpha-synuclein deposits, vascular parenchymal injury, and hippocampal sclerosis (especially when accompanied by TDP-43 pathology).[35,37]
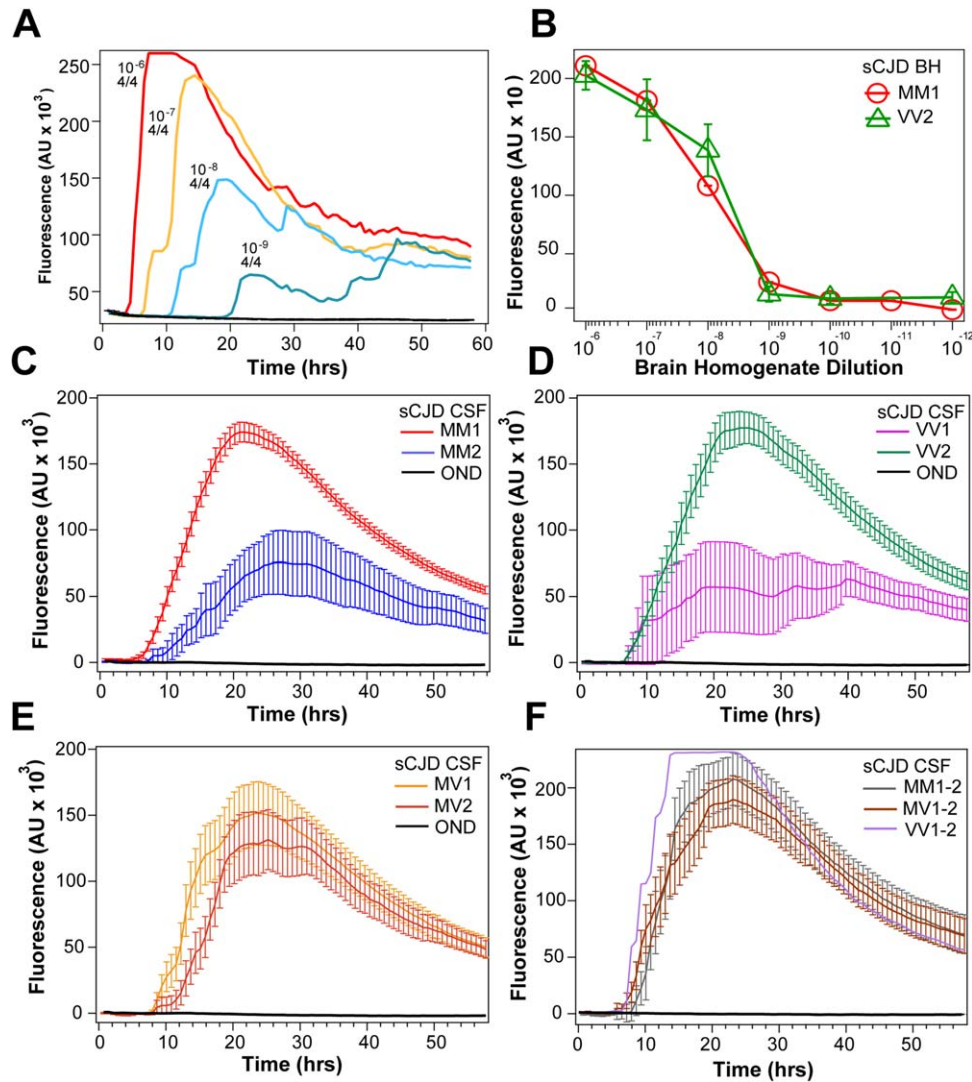
FIGURE 1: Analytical sensitivity and seeding response of second-generation cerebrospinal fluid (CSF) real-time quaking-induced conversion test (RT-QuIC) to major human prions. (A) Serial dilution of brain homogenate (BH) of a typical sporadic Creutz-feldt–Jakob disease (sCJD) MM1 case monitored in real time by thioflavin T fluorescence in second-generation RT-QuIC. The numbers above the RT-QuIC curves denote the dilution and number of positive wells in 4 wells of the assay. (B) Endpoint RT-QuIC sensitivity determined by serial dilutions of BH from 3 cases of sCJD MM1 and sCJD VV2 and monitored with second-generation RT-QuIC (red circles and green triangles). (C) Cumulative plot of second-generation CSF RT-QuIC data obtained in sCJD MM1 (n = 90) and in sCJD MM2 (n = 10). (D) Cumulative plot of CSF RT-QuIC data obtained in sCJD VV1 (n = 7; outlier with no remaining CSF for retesting has been eliminated) and in sCJD VV2 (n = 25). (E) Cumulative plot of CSF RT-QuIC data obtained in sCJD MV1 (n = 15) and in sCJD MV2 (n = 9). (F) Cumulative plot of CSF RT-QuIC data obtained in sCJD MM1-2 (n = 6), sCJD MV1-2 (n = 8), and sCJD VV1-2 (n = 1). The curves are average ± standard deviation of thioflavin T florescence intensity at a given time point. AU = absorbance units; OND = other neurological disorders.

Classification of Cases, Brain Samples, and PRNP Gene Sequencing

DNA was extracted from frozen brain tissues in all cases, and genotypic analysis of the PRNP coding region was performed as described.[12,38,39] On the basis of diagnostic pathology, immunohistochemistry, and WB examination of 2 or 3 brain regions (including frontal, occipital, and cerebellum cortices) with monoclonal antibody 3F4, the pathogenic PrP[Sc] was classified as described previously.[1,30,40,41]

Coronal sections of human brain tissues were obtained at autopsy and stored at −80°C. Three 200 to 350mg cuts of frontal (superior and more posterior middle gyri) cortex were

taken from each brain and used for molecular analyses. The other symmetric cerebral hemisphere was fixed in formalin and used for neuropathological classification of prion disease using histological and immunohistochemical analysis of samples from 16 anatomical areas and NPDPSC's standard protocols.[1,42,43] In a case of equivocal classification of sCJD subtype between pathology and WB, we based the classification on the molecular characteristics of PrP[Sc] on WB developed with a panel of antibodies specific for type 1 and type 2 as described previously.[1,44,45] These criteria allowed the classification of all cases.

CSF Samples

CSF samples were referred to the NPDPSC from US medical institutions that had patients with suspected CJD or other prion diseases. All CSF samples were shipped on dry ice, tested for t-tau and 14-3-3 proteins, and stored at −80°C. In the retrospective study, those with an autopsy-confirmed diagnosis of prion disease or an autopsy-confirmed nonprion disease diagnosis were selected for second-generation RT-QuIC analysis, and cases were blinded.

Controls

Each RT-QuIC plate contained a positive control run in quadruplicate, a negative control run in octuplicate, and up to 21 CSF test samples. Positive control wells were seeded with 2μl of sCJD MM1 brain homogenate diluted 5×10^{-6} with 0.1% sodium dodecyl sulfate (SDS)/N2 supplement (Thermo Fisher, Waltham, MA) in phosphate-buffered saline (PBS), and brought to a final reaction volume of 100μl with 13μl of PBS. Negative control wells were seeded with 15μl of PBS. Testing wells were seeded with 15μl of neat CSF from patients with an autopsy-confirmed diagnosis of CJD or an autopsy-confirmed nonprion disease diagnosis.

Preparation of Recombinant PrP

N-terminally truncated Syrian hamster recombinant PrP (SHarPrP[90-231]) was prepared as previously described[31,46] with minor modifications. Briefly, recombinant protein purification was performed using an AKTA Prime Plus system (GE Life Sciences, Marlborough, MA) with the addition of a column prewashing step. In this step, denaturing buffer (100mM sodium phosphate [pH 8.0], 10mM Tris, 6 M Guanidine-HCl) was passed through the column at 2.3ml/min for 30 minutes prior to protein gradient refolding. Protein concentration was determined using a Nano-Drop Lite Spectrophotometer (Thermo Scientific, Wilmington, DE) with absorbance measured at 280nm. Purity of SHaPrP(90-231) was ≥95%, as estimated by Coomassie staining after SDS–polyacrylamide gel electrophoresis and by immunoblotting. Analytical sensitivity and bioactivity of purified SHarPrP(90-231) were tested via the second-generation RT-QuIC assay.

Second-Generation RT-QuIC

The second-generation RT-QuIC assays[31] were performed as previously described, with minor modifications. The RT-QuIC reaction mix was prepared as follows: 10mM phosphate buffer (pH 7.4), 300mM NaCl, 0.1mg/ml SHarPrP(23-231), 10μM ThT, 1mM ethylenediaminetetraacetic acid tetrasodium salt, and 0.002% SDS. The 85μl of reaction mix was loaded into each plate well and seeded with 15μl of neat CSF for a final reaction volume of 100μl. The incubation and real-time fluorescence monitoring were performed using the FLUOstar Omega plate reader (BMG Labtech, Ortenberg, Germany) set to the following parameters: 55°C incubation, 60-hour reaction time, 60-second shake/60-second rest cycles, with ThT fluorescence measurements taken every 45 minutes.

RT-QuIC Data Analysis

To condense the large amount of raw RT-QuIC data for analysis, the average maximum ThT relative fluorescence units of
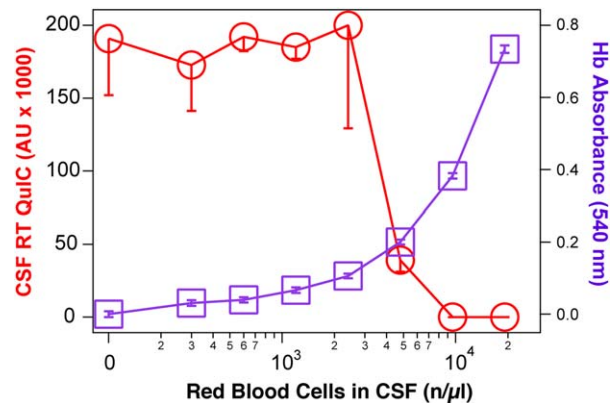

FIGURE 2: Effect of blood contamination on second-generation cerebrospinal fluid (CSF) real-time quaking-induced conversion test (RT-QuIC). Human blood was diluted into positive CSF samples received from patients with variable sporadic Creutzfeldt–Jakob disease (sCJD) subtypes: sCJD VV2 (n = 3), sCJD MM1 (n = 3), sCJD MV1 (n = 2), MV1-2 (n = 1), and generic CJD with the E200K mutation (n = 1); and the second-generation CSF RT-QuIC was performed as described. Red blood cells (RBCs) were counted before disruption by freezing and thawing, followed by in-plate absorbance reading for hemoglobin (Hb) at 540nm. The curves are average ± standard deviation of thioflavin T florescence intensity in CSF RT-QuIC *(red circles)* and hemoglobin (Hb) absorbance *(purple squares)* at a given RBC count. AU = arbitrary fluorescence units.

quadruple positive control (P_{max}), individual CSF sample quadruples (S_{max}), and no seed control octuplicates (N_{max}) were calculated. To compensate for variations in baselines between individual samples and relative fluorescence readings between plate readers, a baseline correction was performed in which the N_{max} value was subtracted from both P_{max} and S_{max} values. Baseline-corrected S_{max} values were then normalized as a percentage of P_{max}. Normalized values were calculated by dividing baseline-corrected S_{max} by baseline-corrected P_{max} and multiplying by 100. The samples were considered positive if >1 well in the first round or 2 wells total, in first and repeat rounds, were positive and exceeded the diagnostic cutoff calculated as a mean ± 4 standard deviations (SD) of all autopsy prion-negative cases.

Tolerance of Second-Generation RT-QuIC to Blood Contamination

A human blood sample with a known red blood cell (RBC) count was serially diluted with PBS. Eight dilutions ranging from 300 to 38,400 cells/μl were aliquoted into 1ml aliquots and stored at −80°C. A 1ml aliquot of each dilution was removed from the freezer, allowed to thaw, and diluted 1:1 with a known RT-QuIC–positive and RT-QuIC–negative CSF sample. The final concentration of RBCs in spiked CSF samples ranged from 150 to 19,600 cells/μl. Blood-spiked CSF samples were spun at $2,000 \times g$ for 2 minutes and loaded onto a 96-well plate, and their absorbance was read at 540nm in a FLUOstar plate reader (BMG Labtech). The seeding activity of each blood-spiked CSF was assessed via RT-QuIC, and the maximum allowed tolerance was determined.

TABLE 1. Demographics, Cerebrospinal Fluid Data, Neuropathological Classification, and Clinical Profiles of Retrospective Cohort

Prion Disease Origin	Unit	Neuropathological Classification										Total
		Sporadic							Genetic			
		MM1	MV1	MV2	VV1	VV2	MM2-C	sFI	gCJD	GSS	FFI	
Total	No.	61	10	9	8	15	7	1	12	2	1	126
	(%)	(48.4)	(7.9)	(7.1)	(6.3)	(11.9)	(5.6)	(0.8)	(9.5)	(1.6)	(0.8)	(100)
Age at death	yr	67.7	70.4	68.3	61.9	63.6	64.9	60.0	57.5	60.0	61.0	65.8
	[SD]	[9.8]	[6.4]	[5.0]	[15.8]	[9.7]	[20.8]	[0.0]	[8.4]	[11.3]	[0.0]	[10.9]
Duration	mo	3.4	9.4	14.2	6.9	6.4	12.5	13.0	3.5	30.9	9.4	6.4
	[SD]	[2.7]	[0.0]	[9.6]	[2.6]	[3.6]	[11.7]	[0.0]	[2.4]	[0.1]	[0.0]	[6.9]
Male	No.	28	4	6	5	8	4	1	8	1	1	66
	(%)	(45.9)	(40.0)	(66.7)	(62.5)	(66.7)	(50.0)	(100.0)	(66.7)	(50.0)	(100.0)	(52.4)
14-3-3 positive	No.	58	9	1	6	15	3	0	10	1	0	103
	(%)	(95.1)	(90.0)	(11.1)	(75.0)	(100.0)	(42.9)	(0.0)	(83.3)	(50.0)	(0.0)	(81.7)
t-Tau positive, >1,150pg/ml	No.	58	9	7	8	15	4	0	11	1	1	114
	(%)	(95.1)	(90.0)	(77.8)	(100.0)	(100.0)	(57.1)	(0.0)	(91.7)	(50.0)	(100.0)	(90.5)
t-Tau	pg/ml	5,071	6,827	2,368	4,177	3,886	2,035	125	6,256	2,974	4,536	4,687
	[SD]	[3,971]	[4,588]	[1,245]	[2,276]	[825]	[1,445]	[0.0]	[5,429]	[3,780]	[0.0]	[3,758]
RT-QuIC positive	No.	58	10	8	6	15	5	0	12	1	1	116
	(%)	(95.1)	(100.0)	(88.9)	(75.0)	(100.0)	(71.4)	(0.0)	(100.0)	(50.0)	(100.0)	(92.1)
PSWCs on EEG (% with EEG results)	No.	14	1	0	0	0	1	—	4	—	0	20
	(%)	(37.8)	(12.5)	(0.0)	(0.0)	(0.0)	(50.0)		(66.7)		(0.0)	(29.4)
Positive MRI (% with MRI results)	No.	36	7	4	7	8	5	1	10	0	0	78
	(%)	(76.6)	(77.8)	(66.7)	(87.5)	(80.0)	(71.4)	(100.0)	(83.3)	(0.0)	(0.0)	(76.5)
Dementia (% with clinical history)	No.	52	8	6	8	11	8	1	11	2	1	108
	(%)	(96.3)	(88.9)	(100.0)	(100.0)	(100.0)	(100.0)	(100.0)	(91.7)	(100.0)	(100.0)	(96.4)
Visual (% with clinical history)	No.	16	3	2	2	3	3	0	2	0	0	31
	(%)	(30.2)	(33.3)	(33.3)	(25.0)	(27.3)	(37.5)	(0.0)	(16.7)	(0.0)	(0.0)	(27.9)
Ataxia (% with clinical history)	No.	34	4	4	5	10	5	0	11	2	1	76
	(%)	(64.2)	(44.4)	(66.7)	(62.5)	(90.9)	(62.5)	(0.0)	(91.7)	(100.0)	(100.0)	(68.5)
Myoclonus (% with clinical history)	No.	24	3	0	6	2	2	0	6	1	1	45
	(%)	(45.3)	(33.3)	(0.0)	(75.0)	(18.2)	(25.0)	(0.0)	(50.0)	(50.0)	(100.0)	(40.5)
Pyramidal Symptoms (% with clinical history)	No.	11	2	3	5	3	2	0	5	1	0	32
	(%)	(20.8)	(22.2)	(50.0)	(62.5)	(27.3)	(25.0)	(0.0)	(41.7)	(50.0)	(0.0)	(28.8)
Extrapyramidal Symptoms (% with clinical history)	No.	11	6	3	4	1	1	0	3	1	0	30
	(%)	(20.8)	(66.7)	(50.0)	(50.0)	(9.1)	(12.5)	(0.0)	(25.0)	(50.0)	(0.0)	(27.0)

EEG = electroencephalogram; FFI = fatal familial insomnia; gCJD = genetic Creutzfeldt–Jakob disease; GSS = Gerstmann–Sträussler–Scheinker disease; MRI = magnetic resonance imaging; PSWC = periodic sharp wave complex; RT-QuIC = real-time quaking-induced conversion test; SD = standard deviation; sFI = sporadic fatal insomnia.

14-3-3 and Total Tau Analyses

Surrogate markers for prion disease, 14-3-3, and tau protein, were measured by WB and enzyme-linked immunosorbent assay, respectively, as previously described.[20]

CDI

CDI was used to quantify the amount of PrP^{Sc} present in our sCJD (MM1) brain homogenate control and was performed as previously described.[30,41]

Statistical Analysis

The sensitivity, specificity, positive predictive value, negative predictive value, and efficiency of each marker were obtained. The combination of different CSF RT-QuIC data and 14-3-3 or t-tau protein results were tested by two different approaches: (1) positive if both results of CSF RT-QuIC and a second test were positive, and negative if either or both results of CSF RT-QuIC and a second test were negative; and (2) positive if either

TABLE 2. Demographics, Cerebrospinal Fluid Data, Neuropathological Classification, and Clinical Profiles of Prospective Cohort

Prion Disease Origin	Unit	Neuropathological Classification								Genetic	Total
		Sporadic									
		MM1	MV1	VV2	MM2-C	MM1-2	MV1-2	VV1-2	sFI	gCJD	
Total	No.	29	5	11	2	6	8	1	1	2	65
	(%)	(44.6)	(7.7)	(16.9)	(3.1)	(9.2)	(12.3)	(1.5)	(1.5)	(3.1)	
Age at death	yr	69.3	64.4	64.5	66	74.7	66.6	52	61	62	67.5
	[SD]	[7.0]	[9.3]	[8.0]	[4.2]	[11.9]	[5.2]	[0.0]	[0.0]	[0.0]	[8.1]
Duration	mo	3.4	3.6	6.1	8.5	2.9	11.3	28.9	7.5	1.4	5.5
	[SD]	[2.9]	[3.2]	[3.2]	[0.0]	[0.9]	[8.9]	[0.0]	[0.0]	[1.1]	[5.7]
Male	No.	14	4	8	2	1	4	0	1	2	36
	(%)	(48.3)	(80.0)	(72.7)	(100.0)	(16.7)	(50.0)	(0.0)	(100.0)	(100.0)	(55.4)
14-3-3 positive	No.	25	2	11	1	6	5	1	0	2	53
	(%)	(86.2)	(40.0)	(100.0)	(50.0)	(100.0)	(62.5)	(100.0)	(0.0)	(100.0)	(81.5)
t-Tau positive, >1,150pg/ml	No.	28	4	11	2	6	8	1	0	2	62
	(%)	(96.6)	(80.0)	(100.0)	(100.0)	(100.0)	(100.0)	(100.0)	(0.0)	(100.0)	(95.4)
t-Tau	pg/ml	6,278	3,048	8,651	4,681	5,314	3,908	6,793	1,837	7,372	6,067
	[SD]	[4,079]	[3,009]	[2,001]	[5,991]	[2,461]	[2,088]	[0.0]	[0.0]	[462]	[3,528]
RT-QuIC positive	No.	28	4	11	2	6	8	1	0	2	62
	(%)	(96.6)	(80.0)	(100.0)	(100.0)	(100.0)	(100.0)	(100.0)	(0.0)	(100.0)	(95.4)
PSWCs on EEG (% with EEG results)	No. (%)	0 (0.0)	1 (33.3)	0 (0.0)	—	1 (33.3)	0 (0.0)	0 (0.0)	0 (0.0)	0 (0.0)	2 (6.3)
Positive MRI (% with MRI results)	No. (%)	14 (87.5)	3 (60.0)	7 (77.8)	2 (100)	4 (80.0)	4 (57.1)	1 (100)	0 (0.0)	1 (100)	36 (76.6)
Dementia (% with clinical history)	No. (%)	20 (95.2)	5 (100)	9 (100)	2 (100)	5 (100)	8 (100)	1 (100)	1 (100)	1 (100)	52 (98.1)
Visual (% with clinical history)	No. (%)	6 (31.6)	1 (25.0)	4 (44.4)	1 (50.0)	2 (40.0)	1 (14.3)	1 (100)	0 (0.0)	0 (0.0)	16 (32.7)
Ataxia (% with clinical history)	No. (%)	12 (66.7)	1 (33.3)	9 (100)	1 (50.0)	2 (40.0)	6 (85.7)	1 (100)	0 (0.0)	0 (0.0)	32 (68.1)
Myoclonus (% with clinical history)	No. (%)	10 (55.6)	2 (66.7)	3 (37.5)	1 (50.0)	1 (20.0)	2 (28.6)	1 (100)	1 (100)	0 (0.0)	21 (45.7)
Pyramidal Symptoms (% with clinical history)	No. (%)	9 (47.4)	0 (0.0)	2 (25.0)	1 (50.0)	2 (40.0)	3 (42.9)	0 (0.0)	1 (100)	0 (0.0)	18 (38.3)
Extrapyramidal Symptoms (% with clinical history)	No. (%)	3 (16.7)	1 (33.3)	1 (12.5)	0 (0.0)	1 (20.0)	3 (42.9)	0 (0.0)	0 (0.0)	0 (0.0)	9 (19.6)

EEG = electroencephalogram; gCJD = genetic Creutzfeldt–Jakob disease; MRI = magnetic resonance imaging; PSWC = periodic sharp wave complex; RT-QuIC = real-time quaking-induced conversion test; SD = standard deviation; sFI = sporadic fatal insomnia.

or both CSF RT-QuIC and a second test were positive, and negative if results of both CSF RT-QuIC and 14-3-3 were negative. We investigated the effect of the following demographic and laboratory variables on survival: sex, age at onset, and disease duration; and compared the parameters for the whole group and different phenotypic subgroups with analysis of variance (ANOVA) or Fisher exact test. Cumulative survival curves were constructed by the Kaplan–Meier method and compared using the Mantel–Cox and Breslow methods. For each type of

PrP^{Sc} and *PRNP* codon 129 polymorphism, we report descriptive statistics and each variable was compared with ANOVA.

Results

Analytical Sensitivity of Second-Generation RT-QuIC for Human Brain Prions

The analytical sensitivity of second-generation RT-QuIC was determined by serial dilution of brain homogenates

TABLE 3. Retrospective Neuropathological Validation of RT-QuIC

CSF	Unit	Neuropathological Assessment			
		Prion Negative	Prion Positive	sCJD	gCJD
RT-QuIC	No.	67	126	111	15
Specificity	%		98.5	98.5	98.5
Sensitivity	%		92.1	91.9	93.3
PPV	%		99.1	99.0	93.3
NPV	%		86.8	88.0	98.5
14-3-3					
Specificity	%		62.7	62.7	62.7
Sensitivity	%		81.7	82.9	73.3
PPV	%		81.1	79.3	31.4
NPV	%		82.4	87.5	93.3
t-Tau $\geq$ 1,150pg/ml					
Specificity	%		46.3	46.3	46.3
Sensitivity	%		90.5	91.0	86.7
PPV	%		76.0	73.7	26.5
NPV	%		72.1	75.6	93.9

CSF = cerebrospinal fluid; gCJD = genetic Creutzfeldt–Jakob disease; NPV = negative predictive value; PPV = positive predictive value; RT-QuIC = real-time quaking-induced conversion test; sCJD = sporadic Creutzfeldt–Jakob disease.

prepared from 3 typical sCJD MM1 brain samples, 3 sCJD VV2 brain samples, and control cases diagnosed with other neurological diseases (Fig 1A, B). The raw fluorescence kinetic data and dilutions of a typical sCJD MM1 case shown in Figure 1A demonstrate the quantitative RT-QuIC response with progressively diminishing fluorescence signal and extending lag phase. Cumulatively, the second-generation RT-QuIC test demonstrates analytical sensitivity (see Fig 1B) with detection limit for MM1 and VV2 sCJD prions at 10^9-fold dilution of respective brain homogenates. Comparison to PrP^{Sc} levels measured in the initial 10% homogenate with CDI indicated that the endpoint sensitivity of second-generation RT-QuIC is ~3 attograms (ag) of PrP^{Sc} per plate well, corresponding to 10 to 40 prion particles, assuming that the smallest human prion particles with the highest replication potency are composed of 20 to 78 monomers of PrP^{Sc}.[30] In contrast, uniformly flat responses were seen with the unseeded reactions and those reactions seeded with brain homogenates of other neurological diseases.

We investigated the known inhibitory effect[47] of blood contamination on second-generation CSF RT-QuIC by serially diluting blood into RT-QuIC–positive CSF samples obtained from patients with variable sCJD subtypes: sCJD VV2 (n = 3), sCJD MM1 (n = 3), sCJD MV1 (n = 2), MV1-2 (n = 1), and gCJD with the E200K mutation (n = 1). We observed a uniform inhibitory effect above 9,600 RBCs/µl corresponding, after freezing and thawing, to the 540nm absorbance of released hemoglobin equal to 0.389. Based on these experiments, we established a threshold (mean − 3 SD) for maximum acceptable blood contamination at hemoglobin absorbance 0.339 corresponding to 8,400 RBC/µl (Fig 2). These criteria excluded 58 (2.7%) of 2,141 tested CSF samples from evaluation.

Diagnostic Performance of Second-Generation CSF RT-QuIC

Autopsy and detailed neuropathological assessment were performed on 272 cases of a total of 2,141 second-generation CSF RT-QuIC tests referred to NPDPSC for evaluation of patients with rapidly progressive neurodegenerative disorders. In the first retrospective RT-QuIC cohort, we blindly tested CJD cases that represented expected frequencies of different prion disease subtypes in the general population.[1] The samples were defined a priori as RT-QuIC positive or negative before unblinding and review of neuropathology.

TABLE 4. Final Neuropathological Diagnosis of Cases with Rapidly Progressive Other Neurological Disorders Clinically Suspected from Prion Disorder

Neuropathological Diagnosis	No.	%
AD	34	41.5
Multi-infarct dementia	7	8.5
AD with multi-infarcts	6	7.3
AD with Lewy bodies	5	6.1
CNS lymphoma	4	4.9
Frontotemporal lobar degeneration	4	4.9
Lewy body dementia	4	4.9
Leukodystrophy	4	4.9
Primary angiitis	2	2.4
Progressive multifocal leukoencephalopathy	2	2.4
Coccidioidomycosis	1	1.2
Diffuse leukoencephalopathy with axonal spheroids	1	1.2
Encephalitis	1	1.2
Focal necrotizing encephalopathy	1	1.2
Global ischemic encephalopathy	1	1.2
Granulomatous amoebic encephalitis	1	1.2
Hemorrhagic stroke	1	1.2
Leptomeningeal carcinomatosis	1	1.2
Malignant glioma	1	1.2
Wernicke–Korsakoff syndrome with olivary gliosis	1	1.2
Undetermined	1	1.2
Total	82	100

AD = Alzheimer disease; CNS = central nervous system.

Other rapidly progressive neurological disorders, most frequently rapidly progressive AD, were used as control cases.[23,48] The samples that were previously tested for 14-3-3 and t-tau proteins were blinded and tested with second-generation CSF RT-QuIC. The demographics, and clinical and neuropathological classification of the retrospective cohort are summarized in Table 1. The neuropathologically verified RT-QuIC–positive cases were associated with older age ($p = 0.002$), shorter disease course ($p = 0.014$), and

higher frequency of ataxia ($p = 0.034$). The RT-QuIC was more frequently negative in sCJD MM2 ($p = 0.024$), and we observed no correlation of the RT-QuIC result with the origin (sporadic or genetic) of prion disease, codon 129 polymorphism alone, gender, electroencephalogram, and MRI.

To evaluate the second-generation CSF RT-QuIC performance during routine CSF testing, we blindly tested all samples sent to NPDPSC with RT-QuIC and in parallel for 14-3-3 and t-tau proteins. All data were decoded and evaluated after autopsy, neuropathological assessment, and *PRNP* gene sequencing. Comparing the retrospective and prospective prion cohort (Table 2), the data indicate a greater preponderance of rapidly progressive prion diseases with shorter illness duration and 23% were mixed PrP^{Sc} type 1-2 cases that were not incorporated into the retrospective study.

The general diagnostic performance of second-generation CSF RT-QuIC, in the retrospective cohort, is superior to both traditional 14-3-3 and t-tau surrogate tests (Table 3). The 98.5% diagnostic specificity in all prion disease forms is due to one case, which repeatedly tested positive in CSF RT-QuIC, but which after the neuropathology was found to be Lewy body dementia (LBD). However, after precipitating prions from brain homogenate with phosphotungstic acid (PTA) followed by WB and CDI,[30,41] we observed low, but above treshhold levels of PrP^{Sc} that may have escaped detection by immunohistochemistry.[12] Whether this case represents a false positive, or a true positive prion disease carrier with LBD comorbidity will require bioassay. Cumulatively, the increase in diagnostic specificity is particularly clinically relevant in the differential diagnostic clinical category of rapidly progressive dementias, because 42% are malignant forms of AD (Table 4). The prospectively determined diagnostic performance of second-generation CSF RT-QuIC maintains 100% specificity and 95% sensitivity for prion diseases of sporadic and genetic origin, with 100% and 82% positive and negative predictive value, respectively. The diagnostic specificity and sensitivity of both 14-3-3 and t-tau protein were lower than those of CSF RT-QuIC, with 14-3-3 protein being the least reliable indicator of prion disease in all statistical parameters (Table 5 and for individual genetic cases Table 6). Combining the prospective CSF RT-QuIC data with the results of 14-3-3 or t-tau decreased the sensitivity and specificity for CSF RT-QuIC + 14-3-3 protein to 82% and 43%, respectively, and for CSF RT-QuIC + t-tau to 92% and 72%, respectively.

Prion Type Differentiation with Second-Generation CSF RT-QuIC

Cumulative plots of raw data revealed significant differences in the second-generation CSF RT-QuIC patterns,

CSF	Unit	Neuropathological Assessment			
		Prion Negative	Prion Positive	sCJD	gCJD
RT-QuIC	No.	14	65	63	2
Specificity	%		100.0	100.0	[100.0]
Sensitivity	%		95.4	95.2	[100.0]
PPV	%		100.0	100.0	[100.0]
NPV	%		82.4	82.4	[100.0]
14-3-3					
Specificity	%		42.9	42.9	[42.9]
Sensitivity	%		81.5	81.0	[100.0]
PPV	%		86.9	86.4	[20.0]
NPV	%		50.0	50.0	[100.0]
t-Tau > 1,150pg/ml					
Specificity	%		71.4	71.4	[71.4]
Sensitivity	%		95.4	95.2	[100.0]
PPV	%		93.0	93.8	[33.3]
NPV	%		76.9	76.9	[100.0]

TABLE 5. Prospective Neuropathological Validation of CSF RT-QuIC

All statistical conclusions are based on the separate evaluation of each CSF test. The brackets indicate weak CSF data statistics due to the limited number of gCJD cases.

CSF = cerebrospinal fluid; gCJD = genetic Creutzfeldt–Jakob disease; NPV = negative predictive value; PPV = positive predictive value; RT-QuIC = real-time quaking-induced conversion test; sCJD = sporadic Creutzfeldt–Jakob disease.

in both maximum fluorescence and lag interval, obtained in different subtypes of sCJD cases (see Fig 1). All the sCJD MM1 cases showed a significantly shorter lag phase and higher maximum fluorescence values than sCJD MM2 cases ($p < 0.0001$). In contrast, the sCJD VV1 cases showed significantly lower fluorescence intensity and an extended lag phase ($p = 0.0011$). Neither parameter differentiated CSF RT-QuIC of heterozygous sCJD MV1 from MV2, and the average fluorescence intensity was intermediate. Interestingly, the cases with mixed type 1-2 PrP^{Sc} in the same or different brain locations generated patterns of CSF RT-QuIC similar to those of sCJD MM1, reminiscent of the previous observation in protein misfolding cyclic amplification (PMCA), in which type 1 prions progressively won the replication competition with the more slowly replicating type 2 prions.[40] With the cutoff value for maximum fluorescence intensity of sCJD MM2 set at mean + 3 SD, the individual CSF RT-QuIC data allowed differentiation of sCJD MM1 from sCJD MM2 with 95% probability. The higher RT-QuIC seeding potency of sCJD MM1 cases correlated with only a 2.7-month median cumulative survival and contrasted significantly with the median 9.7-month survival of MM2 cases ($p = 0.015$; Fig 3A, B). Similarly, the CSF RT-QuIC fluorescence intensity differentiated sCJD VV1 from sCJD VV2 with 80% probability (see Fig 3C, D). The previously reported survival data indicated significantly longer survival of sCJD VV1 compared to sCJD VV2 cases,[1,49] but this trend was not significant in our subset due to the small number of cases. Cases of gCJD, GSS, and FFI had clearly different seeding effects in CSF RT-QuIC that were unique for each mutation. Whereas gCJD with E200K mutation tested in CSF RT-QuIC was invariably highly positive, the CSF RT-QuIC seeding activity varied widely with each specific mutation in GSS and in FFI, and these data correlate with the broad variation in disease duration (see Fig 3E, F).

Discussion

Neuropathological evaluation of the cases from this retrospective and prospective study show that second-generation RT-QuIC analysis of CSF samples from

TABLE 6. Neuropathological Classification, *PRNP* Gene Sequencing, and Cerebrospinal Fluid Data in Individual Patients with Genetic Prion Diseases

Classification	*PRNP* Gene Mutation, Codon 129, and Chromosomal Configuration	RT-QuIC	14-3-3	Tau > 1,150pg/ml	Tau, pg/ml
gCJD	p.E200K-p.129M (p.129M/M)	+	−	+	2,576
gCJD	p.E200K-p.129M (p.129M/M)	+	+	+	2,942
gCJD	p.E200K-p.129M (p.129M/M)	+	+	+	4,564
gCJD	p.E200K-p.129M (p.129M/M)	+	+	+	3,811
gCJD	p.E200K-p.129M (p.129M/M)	+	+	+	7,698
gCJD	p.E200K-p.129M (p.129M/M)	+	+	+	7,045
gCJD	p.E200K-p.129M (p.129M/M)	+	+	+	7,698
gCJD	p.E200K-p.129M (p.129M/M)	+	+	+	7,045
gCJD	p.E200K-p.129M (p.129M/M)	+	+	+	6,627
gCJD	p.E200K-p.129V (p.129M/V)	+	+	+	20,360
gCJD	p.E200K-p.129M (p.129M/V)	+	−	−	991
gCJD	p.E200K-p.129V (p.129V/V)	+	+	+	4,033
gCJD	p.V210I-p.129M (p.129M/M)	+	+	+	4,180
gCJD	p.V210I-p.129M (p.129M/M)	+	+	+	8,468
FFI	p.D178N-p.129M (p.129M/M)	+	−	+	4,536
GSS	p.A117V-p.129V (p.129V/V)	−	−	−	301
GSS	p.P102L-p.1296M (p.129M/M)	+	+	+	5,647

FFI = fatal familial insomnia; gCJD = genetic Creutzfeldt–Jakob disease; GSS = Gerstmann–Sträussler–Scheinker disease; RT-QuIC = real-time quaking-induced conversion test.

patients with suspected prion diseases can detect prions with a specificity and sensitivity of 98.5 to 100% and 92 to 95%, respectively. The high diagnostic specificity compares well with the results of the earlier version of RT-QuIC.[47,50,51] However, high analytical sensitivity with a detection limit of 3ag of pathogenic PrP[Sc], corresponding to 10 to 40 human prion particles, leads to enhanced diagnostic sensitivity and reproducibility. Consequently, second-generation RT-QuIC missed only 5 to 8% of prion cases compared to 11 to 23% in the first-generation assays.[31,47,50–52]

The results from this study show that the second-generation CSF RT-QuIC has, in a standard surveillance setting, higher sensitivity and specificity to CSF 14-3-3 (monitored here with WB) and t-tau proteins. Combining the CSF results into a 2-component panel did not increase diagnostic sensitivity, but significantly decreased the specificity of the final conclusion. However, further

studies are required to assess the complementary role, if any, which CSF 14-3-3 or t-tau on the one hand, and CSF second-generation CSF RT-QuIC on the other, may play in the differential clinical diagnosis of neurodegenerative diseases. The observed lower specificity of 14-3-3 protein and higher specificity of t-tau in the prospective cohort may reflect a higher proportion of rapidly progressive nonprion cases in this cohort, the trend already noticed in an earlier study.[53] However, to draw a definitive conclusion would require expanding the numbers of prospectively followed autopsied cases. Ongoing studies are being pursued and more CSF samples need to be investigated from patients with variant CJD, gCJD, variably protease-sensitive prionopathy, and other atypical prion diseases so that a better understanding can emerge of how this new test can be used in detection and differentiation of the less common and often atypical prion diseases.
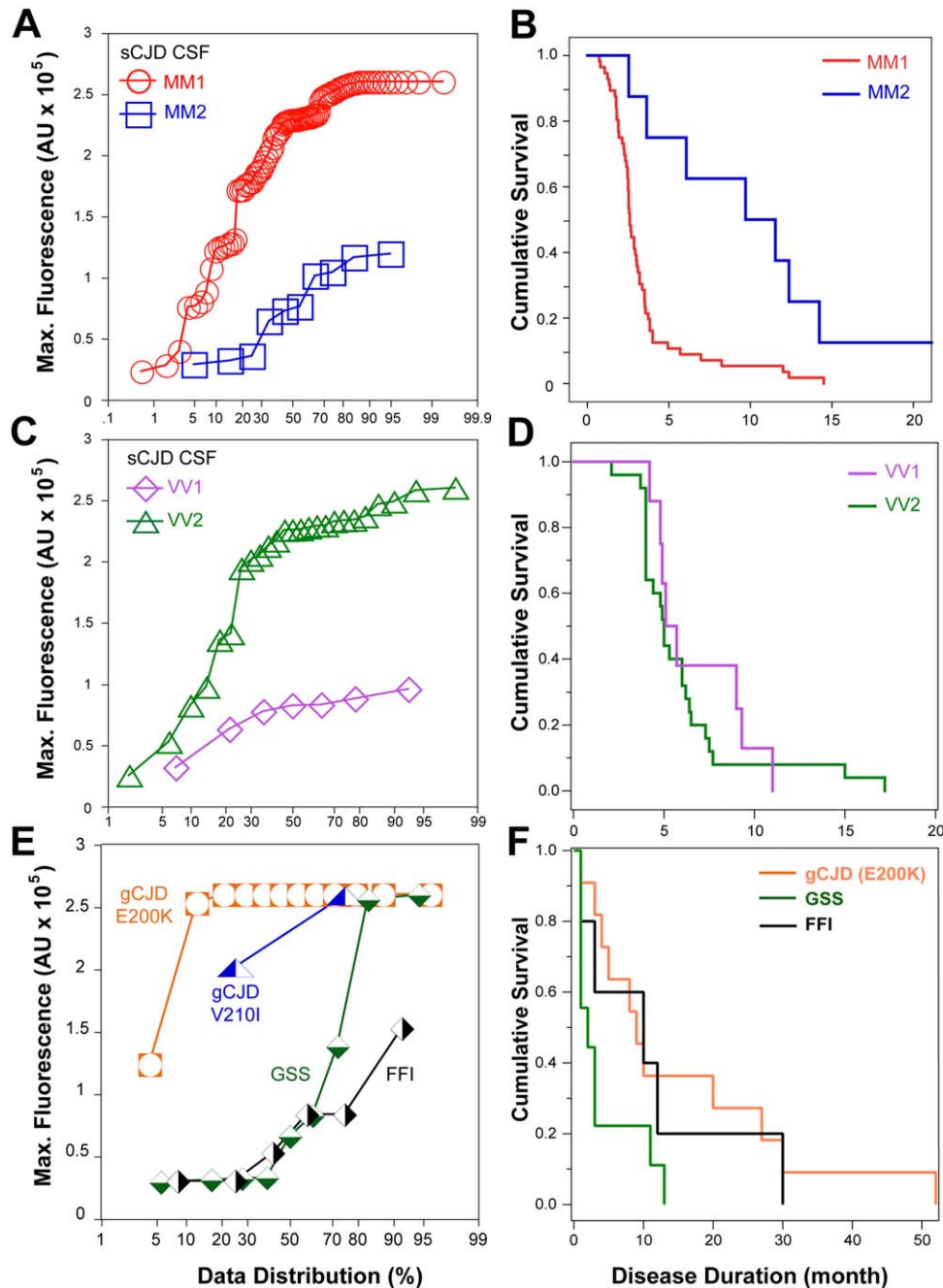
FIGURE 3: Differentiation of major human prion subtypes based on seeding potency in second-generation cerebrospinal fluid (CSF) real-time quaking-induced conversion test (RT-QuIC) and relationship with the disease progression rate. (A) Individual data distribution of maximum CSF second-generation RT-QuIC fluorescence obtained in sporadic Creutzfeldt–Jakob disease (sCJD) MM1 (n = 90) and sCJD MM2 (n = 10). (B) Cumulative survival curves of sCJD cases plotted in A. (C) Cumulative plot of CSF RT-QuIC data obtained in sCJD VV1 (n = 7; outlier with no remaining CSF for retesting is not plotted) and in sCJD VV2 (n = 25). (D) Cumulative survival curves of sCJD cases plotted in C. (E) Cumulative plot of CSF RT-QuIC data obtained in genetic prion disease (genetic Creutzfeldt–Jakob disease [gCJD]; E200K, n = 12; V210I, n = 2), Gerstmann–Sträussler–Scheinker disease (GSS; n = 9), and fatal familial insomnia (FFI; n = 6). (F) Cumulative survival curves of the genetic prion cases plotted in E. AU = arbitrary fluorescence units.

Interestingly, in the retrospective second-generation CSF RT-QuIC study, we found 1 patient in whom the initial neuropathology was concluded to be LBD but for whom RT-QuIC revealed repeatedly positive CSF for prions. Subsequent reinvestigation of the brain homogenate of this patient after PTA precipitation with CDI and WB revealed low but above-threshold levels of PK-resistant PrP^{Sc}. Considering the up to 50-year incubation time of prion diseases and the high analytical sensitivity of second-generation CSF RT-QuIC, we

conjectured that this patient was likely a subclinical prion carrier who died due to LBD comorbidity. However, a definitive conclusion on this case would require protein misfolding cyclic amplification or bioassay in transgenic mice expressing human or chimeric PrP.[12,25,40]

The analysis of seeding activity kinetics in this study indicates strong agreement between CSF RT-QuIC data and final neuropathological classification after autopsy, which in turn correlates with the cumulative survival and duration of the disease. These correlations allow for the classification and subtyping of prion disease in the majority of cases while the patient is still alive. The CSF RT-QuIC combined with *PRNP* gene sequencing data allowed us to differentiate with 95% probability the most aggressive sCJD MM1 from slowly progressive sCJD MM2, and with 80% probability more aggressive sCJD VV2 prions from CJD VV1 prions, usually associated with slow progression. The 2 negative CSF RT-QuIC findings in cases with sporadic fatal insomnia and 1 case with GSS are intriguing and may suggest either lower levels of prions, distinct prion seeding potency due to the different conformation of PrP^{Sc}, or both. These aspects have to be addressed in parallel investigations of brain tissue to determine the levels and conformational strain characteristics of PrP^{Sc} present in each case.[30,41,54] Although the conversion substrate used in CSF RT-QuIC was Syrian hamster PrP(90-231), nevertheless the seeding activities observed in this study are in general agreement with data we obtained previously with RT-QuIC protocol and human PrP substrate, and PMCA protocol with transgenic mice brain homogenates expressing human PrP^C monitored with CDI.[30,54]

Using advanced biophysical tools, we demonstrated recently that the different molecular characteristics of sCJD prions arise from distinct particle sizes and conformational structure.[14,30,41] Furthermore, our data indicate that phenotypically distinct sCJD prions differ considerably in their structural organization, both at the level of the polypeptide backbone (as indicated by backbone amide hydrogen/deuterium [H/D] exchange data) and in the quaternary packing arrangements (as indicated by H/D exchange kinetics for histidine side chains).[54] Remarkably, the structure of sCJD prions is fundamentally different from that of laboratory rodent prions, and in contrast to previous observations on yeast and some murine prion strains, their replication rate is primarily determined not by conformational stability but by specific structural features that control the growth rate of PrP aggregates.[54] Cumulatively, the second-generation CSF RT-QuIC seems to replicate the conformation-driven seeding aspect of human prion replication remarkably well, and thus accurately predicts the biological characteristics of distinct human prions and establishes the prognosis of the patient. These individualized diagnostic data and prognoses are critical for future therapeutic trials and provide measurable objective criteria for therapeutic efficacy.

Acknowledgment

Author Contributions

A.F., C.H., and J.G.S. were responsible for conception and design of the study. All authors were responsible for acquisition and analysis of data. A.F., B.S.A., and J.G.S. were responsible for drafting of the manuscript and figures.

Potential Conflicts of Interest

Nothing to report.

References

1. Puoti G, Bizzi A, Forloni G, et al. Sporadic human prion diseases: molecular insights and diagnosis. Lancet Neurol 2012; 11:618–628.

2. Prusiner SB. Scrapie prions. Annu Rev Microbiol 1989;43:345–374.

3. Prusiner SB, Scott MR, DeArmond SJ, Cohen FE. Prion protein biology. Cell 1998;93:337–348.

4. Bruce ME, McBride PA, Farquhar CF. Precise targeting of the pathology of the sialoglycoprotein, PrP, and vacuolar degeneration in mouse scrapie. Neurosci Lett 1989;102:1–6.

5. Hecker R, Taraboulos A, Scott M, et al. Replication of distinct scrapie prion isolates is region specific in brains of transgenic mice and hamsters. Genes Dev 1992;6:1213–1228.

6. Bessen RA, Marsh RF. Distinct PrP properties suggest the molecular basis of strain variation in transmissible mink encephalopathy. J Virol 1994;68:7859–7868.

7. Telling GC, Parchi P, DeArmond SJ, et al. Evidence for the conformation of the pathologic isoform of the prion protein enciphering and propagating prion diversity. Science 1996;274: 2079–2082.

8. Safar J, Wille H, Itri V, et al. Eight prion strains have PrP^{Sc} molecules with different conformations. Nat Med 1998;4:1157–1165.

9. Peretz D, Scott M, Groth D, et al. Strain-specified relative conformational stability of the scrapie prion protein. Protein Sci 2001;10: 854–863.

10. Legname G, Baskakov IV, Nguyen H-OB, et al. Synthetic mammalian prions. Science 2004;305:673–676.

11. Parchi P, Giese A, Capellari S, et al. Classification of sporadic Creutzfeldt-Jakob disease based on molecular and phenotypic analysis of 300 subjects. Ann Neurol 1999;46:224–233.

12. Safar JG, Geschwind MD, Deering C, et al. Diagnosis of human prion disease. Proc Natl Acad Sci U S A 2005;102: 3501–3506.

13. Bai HX, Zou Y, Lee AM, et al. Diagnostic value and safety of brain biopsy in patients with cryptogenic neurological disease: a systematic review and meta-analysis of 831 cases. Neurosurgery 2015;77:283–295; discussion 295.

14. Safar JG. Molecular mechanisms encoding quantitative and qualitative traits of prion strains. In: Gambetti P, ed. Prions and diseases. New York, NY: Springer Verlag, 2012: 161–179.

15. Zerr I, Kallenberg K, Summers DM, et al. Updated clinical diagnostic criteria for sporadic Creutzfeldt-Jakob disease. Brain 2009; 132(pt 10):2659–2668.

16. Forner SA, Takada LT, Bettcher BM, et al. Comparing CSF biomarkers and brain MRI in the diagnosis of sporadic Creutzfeldt-Jakob disease. Neurol Clin Pract 2015;5: 116–125.

17. Geschwind MD, Martindale J, Miller D, et al. Challenging the clinical utility of the 14-3-3 protein for the diagnosis of sporadic Creutzfeldt-Jakob disease. Arch Neurol 2003;60:813–816.

18. Sanchez-Juan P, Green A, Ladogana A, et al. CSF tests in the differential diagnosis of Creutzfeldt-Jakob disease. Neurology 2006; 67:637–643.

19. Sanchez-Juan P, Sanchez-Valle R, Green A, et al. Influence of timing on CSF tests value for Creutzfeldt-Jakob disease diagnosis. J Neurol 2007;254:901–906.

20. Hamlin C, Puoti G, Berri S, et al. A comparison of tau and 14-3-3 protein in the diagnosis of Creutzfeldt-Jakob disease. Neurology 2012;79:547–552.

21. Schmitz M, Ebert E, Stoeck K, et al. Validation of 14-3-3 protein as a marker in sporadic Creutzfeldt-Jakob disease diagnostic. Mol Neurobiol 2016;53:2189–2199.

22. Karch A, Hermann P, Ponto C, et al. Cerebrospinal fluid tau levels are a marker for molecular subtype in sporadic Creutzfeldt-Jakob disease. Neurobiol Aging 2015;36:1964–1968.

23. Chitravas N, Jung RS, Kofskey DM, et al. Treatable neurological disorders misdiagnosed as Creutzfeldt-Jakob disease. Ann Neurol 2011;70:437–444.

24. Colby DW, Zhang Q, Wang S, et al. Prion detection by an amyloid seeding assay. Proc Natl Acad Sci U S A 2007;104:20914–20919.

25. Saborio GP, Permanne B, Soto C. Sensitive detection of pathological prion protein by cyclic amplification of protein misfolding. Nature 2001;411:810–813.

26. Atarashi R, Moore RA, Sim VL, et al. Ultrasensitive detection of scrapie prion protein using seeded conversion of recombinant prion protein. Nat Methods 2007;4:645–650.

27. Peden AH, McGuire LI, Appleford NE, et al. Sensitive and specific detection of sporadic Creutzfeldt-Jakob disease brain prion protein using real-time quaking-induced conversion. J Gen Virol 2012;93(pt 2):438–449.

28. Orru CD, Wilham JM, Vascellari S, et al. New generation QuIC assays for prion seeding activity. Prion 2012;6:147–152.

29. Atarashi R, Wilham JM, Christensen L, et al. Simplified ultrasensitive prion detection by recombinant PrP conversion with shaking. Nat Methods 2008;5:211–212.

30. Kim C, Haldiman T, Surewicz K, et al. Small protease sensitive oligomers of PrP(Sc) in distinct human prions determine conversion rate of PrP(C). PLoS Pathog 2012;8:e1002835.

31. Orru CD, Groveman BR, Hughson AG, et al. Rapid and sensitive RT-QuIC detection of human Creutzfeldt-Jakob disease using cerebrospinal fluid. MBio 2015;6(1).

32. WHO infection control guidelines for transmissible spongiform encephalopathies. Geneva, Switzerland: World Health Organization, 1999.

33. Collins SJ, Sanchez-Juan P, Masters CL, et al. Determinants of diagnostic investigation sensitivities across the clinical spectrum of sporadic Creutzfeldt-Jakob disease. Brain 2006;129:2278–2287.

34. Geschwind MD, Shu H, Haman A, et al. Rapidly progressive dementia. Ann Neurol 2008;64:97–108.

35. Cohen ML, Kim C, Haldiman T, et al. Rapidly progressive Alzheimer's disease features distinct structures of amyloid-beta. Brain 2015;138(pt 4):1009–1022.

36. McKhann GM, Knopman DS, Chertkow H, et al. The diagnosis of dementia due to Alzheimer's disease: recommendations from the National Institute on Aging-Alzheimer's Association workgroups on diagnostic guidelines for Alzheimer's disease. Alzheimers Dement 2011;7:263–269.

37. Josephs KA, Nelson PT. Unlocking the mysteries of TDP-43. Neurology 2015;84:870–871.

38. Parchi P, Zou W, Wang W, et al. Genetic influence on the structural variations of the abnormal prion protein. Proc Natl Acad Sci U S A 2000;97:10168–10172.

39. Parchi P, Castellani R, Capellari S, et al. Molecular basis of phenotypic variability in sporadic Creutzfeldt-Jakob disease. Ann Neurol 1996;39:767–778.

40. Haldiman T, Kim C, Cohen Y, et al. Co-existence of distinct prion types enables conformational evolution of human PrPSc by competitive selection. J Biol Chem 2013;288:29846–29861.

41. Kim C, Haldiman T, Cohen Y, et al. Protease-sensitive conformers in broad spectrum of distinct PrP structures in sporadic Creutzfeldt-Jakob disease are indicator of progression rate. PLoS Pathog 2011;7:e1002242.

42. Kim JI, Cali I, Surewicz K, et al. Mammalian prions generated from bacterially expressed prion protein in the absence of any mammalian cofactors. J Biol Chem 2010;285:14083–14087.

43. Gambetti P, Kong Q, Zou W, et al. Sporadic and familial CJD: classification and characterisation. Br Med Bull 2003;66:213–239.

44. Parchi P, de Boni L, Saverioni D, et al. Consensus classification of human prion disease histotypes allows reliable identification of molecular subtypes: an inter-rater study among surveillance centres in Europe and USA. Acta Neuropathol 2012;124:517–529.

45. Cali I, Castellani R, Alshekhlee A, et al. Co-existence of scrapie prion protein types 1 and 2 in sporadic Creutzfeldt–Jakob disease: its effect on the phenotype and prion-type characteristics. Brain 2009;132:2643–2658.

46. Wilham JM, Orru CD, Bessen RA, et al. Rapid end-point quantitation of prion seeding activity with sensitivity comparable to bioassays. PLoS Pathog 2010;6:e1001217.

47. Cramm M, Schmitz M, Karch A, et al. Stability and reproducibility underscore utility of RT-QuIC for diagnosis of Creutzfeldt-Jakob disease. Mol Neurobiol 2016;53:1896–1904.

48. Cohen M, Appleby B, Safar JG. Distinct prion-like strains of amyloid beta implicated in phenotypic diversity of Alzheimer's disease. Prion 2016;10:9–17.

49. Pocchiari M, Puopolo M, Croes EA, et al. Predictors of survival in sporadic Creutzfeldt-Jakob disease and other human transmissible spongiform encephalopathies. Brain 2004;127(pt 10):2348–2359.

50. McGuire LI, Peden AH, Orru CD, et al. Real time quaking-induced conversion analysis of cerebrospinal fluid in sporadic Creutzfeldt-Jakob disease. Ann Neurol 2012;72:278–285.

51. Cramm M, Schmitz M, Karch A, et al. Characteristic CSF prion seeding efficiency in humans with prion diseases. Mol Neurobiol 2015;51:396–405.

52. Atarashi R, Satoh K, Sano K, et al. Ultrasensitive human prion detection in cerebrospinal fluid by real-time quaking-induced conversion. Nat Med 2011;17:175–178.

53. Stoeck K, Sanchez-Juan P, Gawinecka J, et al. Cerebrospinal fluid biomarker supported diagnosis of Creutzfeldt-Jakob disease and rapid dementias: a longitudinal multicentre study over 10 years. Brain 2012;135(pt 10):3051–3061.

54. Safar JG, Xiao X, Kabir ME, et al. Structural determinants of phenotypic diversity and replication rate of human prions. PLoS Pathog 2015;11:e1004832.